Chaos, Solitons and Fractals 110 (2018) 76–81

Contents lists available at ScienceDirect

Chaos, Solitons and Fractals

Nonlinear Science, and Nonequilibrium and Complex Phenomena

journal homepage: www.elsevier.com/locate/chaos

Noise-induced bursting and chaos in the two-dimensional Rulkov model

Irina Bashkirtseva, Venera Nasyrova, Lev Ryashko*

Institute of Natural Science and Mathematics, Ural Federal University, Pr. Lenina 51, Ekaterinburg 620000, Russia

A R T I C L E I N F O

Article history:
Received 23 November 2017
Accepted 4 March 2018
Available online 16 March 2018

Keywords:
Bursting
Chaos
Neural activity
Rulkov model
Stochastic excitement

A B S T R A C T

We study an effect of random disturbances on the discrete two-dimensional Rulkov neuron model. We show that close to the Neimark–Sacker bifurcation, the increasing noise can cause the transition from the noisy quiescence with small-amplitude oscillations near the stable equilibria to the stochastic bursting with large-amplitude spikes. Mean values and variations of the interspike intervals are studied in dependence of the noise intensity. To study the noise-induced bursting, the analytical approach based on the stochastic sensitivity functions technique and confidence ellipses method is applied. On the basis of the largest Lyapunov exponents, we show how the noise-induced transition from the quiescence to stochastic bursting regime is accompanied by the transformation of dynamics from regular to chaotic.

1. Introduction

In the actively developing field of research related to biological modeling, a special role is played by the study of dynamic models of the neuronal activity. These models reflect a wide diversity of the regimes of the neuronal activity, and therefore possess complex excitable attractors and exhibit unexpected nonlinear phenomena [1–3]. The continuous-time models, such as Fitzhugh–Nagumo [4–8], Hodgkin–Huxley [9–13], Morris–Lecar [14–17] and Hindmarsh–Rose [18–23] models, were extensively studied by many authors in both deterministic and stochastic cases. While the theory of continuous-time neuron models using differential equations has been widely developed, less attention has been devoted to the study of map-based discrete-time models [24].

The discrete-time Rulkov system [25] was one of the first phenomenological models which demonstrate basic types of the neural activity, such as the quiescence, the tonic spiking and bursting. Mathematically, the two-dimensional Rulkov model exhibits various bifurcations and attractors [26,27]. This model is actively used in the study of the dynamics of neural networks [28–31]. Even in the one-dimensional case, the Rulkov model exhibits interesting phenomena under the influence of random disturbances [32].

The aim of the present paper is to study how the two-dimensional Rulkov model responds to random perturbations. Our analysis is focused on the parametric zone near the Neimark–Sacker bifurcation.

An analysis of the stochastic phenomena in the map-based dynamical systems attracts attention of many researchers (see, e.g.[33–36]). However, until now the main research method is the direct numerical simulation of the random trajectories that is time-consuming in the parametric study. A rigorous theoretical description of the dynamics of probabilistic distributions of solutions of the stochastic discrete systems is given by the Perron–Frobenius equation [36]. An analytical solution of such functional equations is available only in the exceptional cases. A constructive method of the approximation of the probabilistic distributions based on the stochastic sensitivity functions (SSF) technique has been proposed in [37]. In the present paper, we apply this technique to the analysis of the noise-induced bursting in the two-dimensional Rulkov model. A short overview of the stochastic sensitivity function technique and method of the confidence ellipses is given in the Appendix.

The present paper is organized as follows.

In Section 2, we give a short summary of dynamical regimes for the deterministic 2D Rulkov model in the zone of the Neimark–Sacker bifurcation connected with the loss of stability of the equilibrium and birth of the stable invariant curve. In the zone of stable equilibria, sub- and superthreshold regimes are discussed. In the zone of the stable closed invariant curves, a phenomenon of the Canard explosion is illustrated.

Section 3 is devoted to the study of the noise-induced generation of the stochastic bursting in the zone where the initial deterministic model has the stable equilibrium as a single attractor. We show how under increasing noise the system transforms from the noisy quiescence with the small-amplitude stochastic oscilla-

* Corresponding author.
E-mail address: lev.ryashko@urfu.ru (L. Ryashko).

https://doi.org/10.1016/j.chaos.2018.03.011
0960-0779/

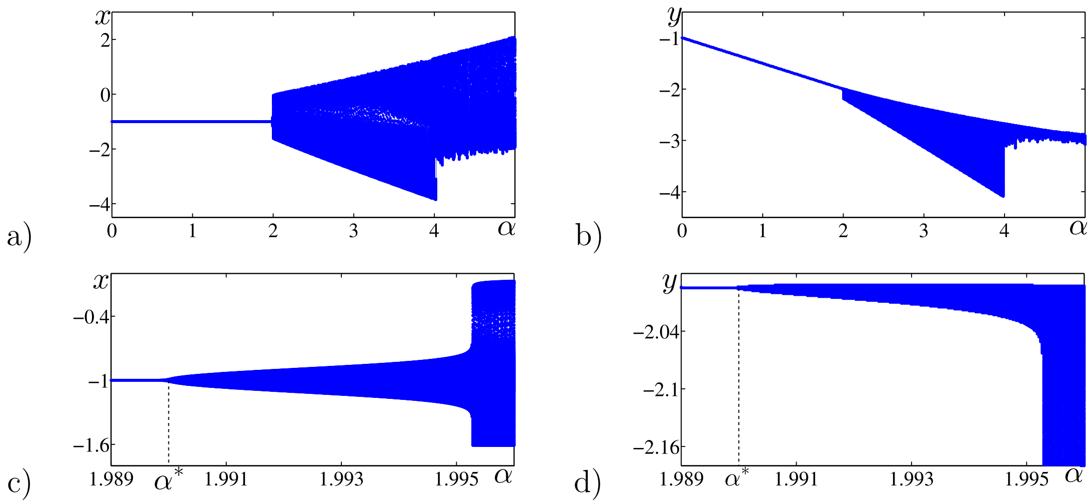

Fig. 1. Bifurcation diagram of the deterministic system (1) with $\sigma = \beta = 0.005$. Enlarged fragments are shown in the bottom panel.

tions to the bursting with large-amplitude stochastic spikes. Here, for the data of the direct numerical simulations, statistics of inter-spike intervals are analyzed.

In Section 4, for the analysis of the geometric probabilistic mechanisms of the noise-induced generation of the bursting, the stochastic sensitivity function technique and the method of the confidence ellipses is used. We show that the onset of the bursting in the case of stable equilibria can be predicted by the analysis of the mutual arrangement of the confidence ellipses and sub- and superthreshold zones. In Section 5, using largest Lyapunov exponents, we show that the noise-induced transition from the quiescence to stochastic bursting regime is accompanied by the transformation of dynamics from regular to chaotic.

2. Deterministic Rulkov model

Consider the two-dimensional Rulkov model

$$\begin{cases} x_{t+1} = \dfrac{\alpha}{1+{x_t}^2} + y_t \\ y_{t+1} = y_t - \sigma x_t - \beta \end{cases}, \tag{1}$$

where x and y are fast and slow variables, respectively, and the parameters α, σ and β are positive. In what follows, we will fix $\sigma = \beta = 0.005$ and study a behavior of this system in dependence on the parameter α.

The Rulkov model (1) has a unique equilibrium M with coordinates $\bar{x} = -1, \quad \bar{y} = -1 - \frac{\alpha}{2}$. For this equilibrium, the Jacobi matrix is

$$J = \begin{pmatrix} \dfrac{\alpha}{2} & 1 \\ -0.005 & 1 \end{pmatrix}.$$

The equilibrium M is stable on the interval $0 < \alpha < 1.99$. The parameter value $\alpha^* = 1.99$ corresponds to the point of the Neimark–Sacker bifurcation with the birth of a closed invariant curve. In Fig. 1, the bifurcation diagram of the deterministic model is presented. Here, x- and y-coordinates of attractors are plotted.

The Fig. 2 shows the phase portraits of the deterministic system (1) for the $\alpha = 1.9$ and $\alpha = 1.98$ in the zone of stable equilibria. As can be seen, if the deviation of the starting point from the equilibrium is small, then the trajectory quickly relaxes to this equilibrium, and a subthreshold response is observed. If the initial deviations is larger than some threshold, the deterministic system exhibits large-amplitude loop before it returns to the small vicinity of the equilibrium and asymptotically tends to M. In this case, the system exhibits a superthreshold response, and a phenomenon of the firing a spike occurs.

Closed invariant curves are shown in Fig. 3 for different values of the parameter $\alpha > \alpha^*$. As can be seen, a size of these closed curves increases when α goes away from the bifurcation point α^*. Note that near $\alpha = 1.995$, a sharp jump of the amplitude values is observed. Such behavior is known as Canard explosion [26]. In the zone of the Canard explosion, both amplitude and the form of these closed invariant curves significantly change. In this regime, system (1) demonstrates a tonic spiking.

In the present paper, we focus on the parameter zone $\alpha < \alpha^*$ and study a response of the equilibria of the Rulkov model to the stochastic forcing.

3. Stochastic excitability of the equilibrium

Consider the stochastically forced two-dimensional Rulkov model

$$\begin{cases} x_{t+1} = \dfrac{\alpha}{1+{x_t}^2} + y_t + \varepsilon_1 \xi_{1,t} \\ y_{t+1} = y_t - \sigma x_t - \beta + \varepsilon_2 \xi_{2,t} \end{cases}, \tag{2}$$

where $\xi_{1,\,t}$, $\xi_{2,\,t}$ are uncorrelated Gaussian random processes with parameters $\mathrm{E}(\xi_{1,t}) = \mathrm{E}(\xi_{2,t}) = 0, \quad \mathrm{E}({\xi^2}_{1,t}) = \mathrm{E}({\xi^2}_{2,t}) = 1$, and ε_1, ε_2 are the noise intensities. In what follows, we put $\varepsilon_1 = \varepsilon_2 = \varepsilon$.

Under the influence of random disturbances, solutions of the stochastic system (2) leave the stable equilibrium M and form a regime of stochastic oscillations. For weak noise, random trajectories are localized near M, and the system (2) exhibits small-amplitude stochastic oscillations (see solutions of system (2) with $\alpha = 1.9$, $\varepsilon = 0.0005$ shown by red in Fig. 4(a) and (b).

For larger noise intensities, the solution of system (2) can fall into the superthreshold zone, and as a result the large-amplitude spike is observed. So, the system exhibits the intermittency of the small- and large-amplitude oscillations. This regime can be interpreted as the noise-induced bursting. This type of the behavior is illustrated in Fig. 4(a) and (b) where solutions of system (2) with $\alpha = 1.9$, $\varepsilon = 0.0008$ are shown by blue color. Note that these noise-induced large-amplitude loops are similar in shape to Canard cycles of the deterministic system (compare Figs. 4(a) and 3).

Such changes in dynamics of system (2) lead to the deformation of the probability density function of random states. In Fig. 4(c), for two values of the noise intensity considered above, plots of the probability density function $\rho(x)$ are shown. For weak noise ($\varepsilon =$

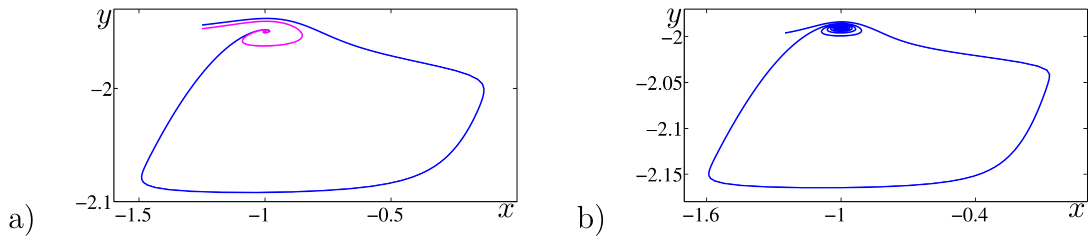

Fig. 2. Phase trajectories of the deterministic system (1) with $\sigma = \beta = 0.005$ for $\alpha = 1.9$ (a), $\alpha = 1.98$ (b).

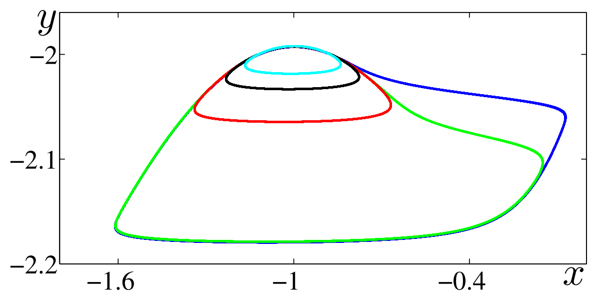

Fig. 3. Closed invariant curves of the deterministic system (1) with $\sigma = \beta = 0.005$ for $\alpha = 1.994$ (light blue), $\alpha = 1.995$ (black), $\alpha = 1.99527$ (red), $\alpha = 1.99528$ (green), $\alpha = 1.996$ (blue). (For interpretation of the references to colour in this figure legend, the reader is referred to the web version of this article.)

0.0005), the curve $\rho(x)$ has one narrow high peak. For $\varepsilon = 0.0008$, this peak becomes lower and wider, and along with it, a new additional peak near $x = -0.15$ appears (see the insert in Fig. 4(c)). So, with the transition to the bursting mode, the shape of the function $\rho(x)$ transforms from unimodal to bimodal. Mathematically, such qualitative change in the probability density function $\rho(x)$ can be interpreted as the stochastic *P*-bifurcation [38]. Details of the transition from the noisy quiescence with small-amplitude stochastic oscillations near the equilibrium *M* to the bursting with the large-amplitude spikes can be seen in Fig. 4(d) where *x*-coordinates of random states are plotted versus noise intensity.

Consider now how the transition to the stochastic bursting occurs for $\alpha = 1.98$ that is closer to the bifurcation point $\alpha^* = 1.99$. In Fig. 5, corresponding results of the simulations are presented. Here, one can see that the onset of the noise-induced bursting is observed for smaller noise than for the case $\alpha = 1.9$.

In the analysis of the noise-induced bursting, the statistics of interspike intervals (ISI) are commonly used. In Fig. 6, mean values *m* and coefficients of variation C_v of ISI are plotted versus ε for three values of the parameter α. The sharp decrease of the function $m(\varepsilon)$ signals about the onset of the stochastic bursting. As can be seen, the closer α to the bifurcation value α^*, the smaller noise generates the stochastic bursting. The coefficient of variation $C_v(\varepsilon)$ is an indicator of the periodicity of the spikes: the smaller the coefficient of variation, the more periodic the spikes are. Note that peaks of C_V in Fig. 6(b) mark intensities of noise which generates the bursting with the maximum variability of ISIs (anti-coherence resonance).

4. Stochastic sensitivity analysis

Let us study the phenomenon of the noise-induced excitability with the help of the stochastic sensitivity function technique and the method of the confidence ellipses. Elements of the stochastic sensitivity matrix $W = \begin{pmatrix} w_{11} & w_{12} \\ w_{21} & w_{22} \end{pmatrix}$ of the equilibrium *M* can be found (see Appendix) analytically:

$$w_{11} = \frac{-40000(100\alpha + 203)}{(100\alpha - 199)(200\alpha + 401)}$$

$$w_{12} = w_{21} = \frac{200(10000\alpha^2 + 100\alpha - 40001)}{(100\alpha - 199)(200\alpha + 401)}$$

$$w_{22} = \frac{-1000000\alpha^3 + 1990000\alpha^2 + 3999900\alpha - 8040201}{(100\alpha - 199)(200\alpha + 401)}.$$

In Fig. 7, eigenvalues $\mu_1(\alpha) > \mu_2(\alpha)$ of the stochastic sensitivity matrix $W(\alpha)$ are plotted. As one can see, as α tends to the bifurcation point α^*, the values of $\mu_{1,2}(\alpha)$ unlimitedly increase. Note that the values $\mu_1(\alpha)$ are two orders of magnitude greater than $\mu_2(\alpha)$.

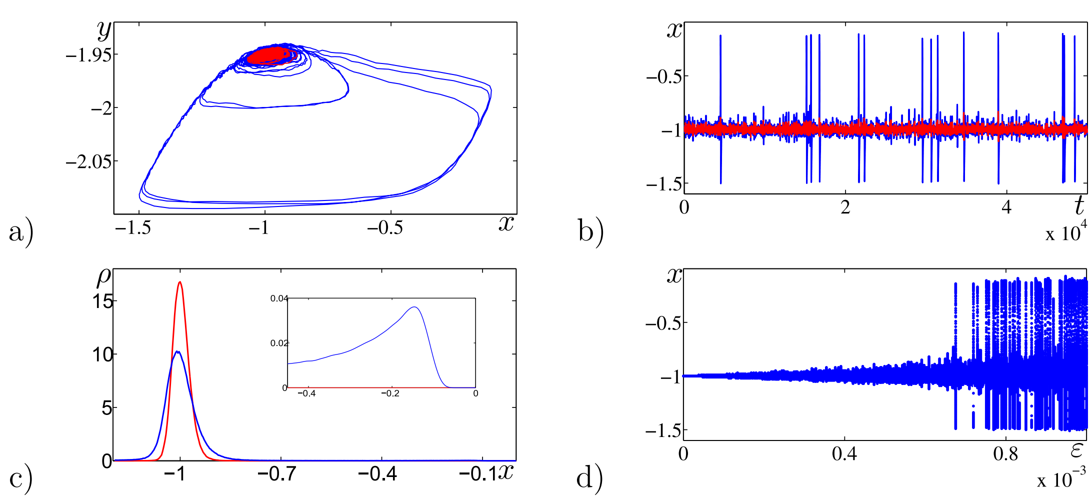

Fig. 4. Stochastic system with $\alpha = 1.9$: (a) random states for $\varepsilon = 0.0005$ (red) and $\varepsilon = 0.0008$ (blue); (b) time series of the variable *x*; (c) probability density of *x*; d) *x*-coordinates of random states versus ε. (For interpretation of the references to colour in this figure legend, the reader is referred to the web version of this article.)

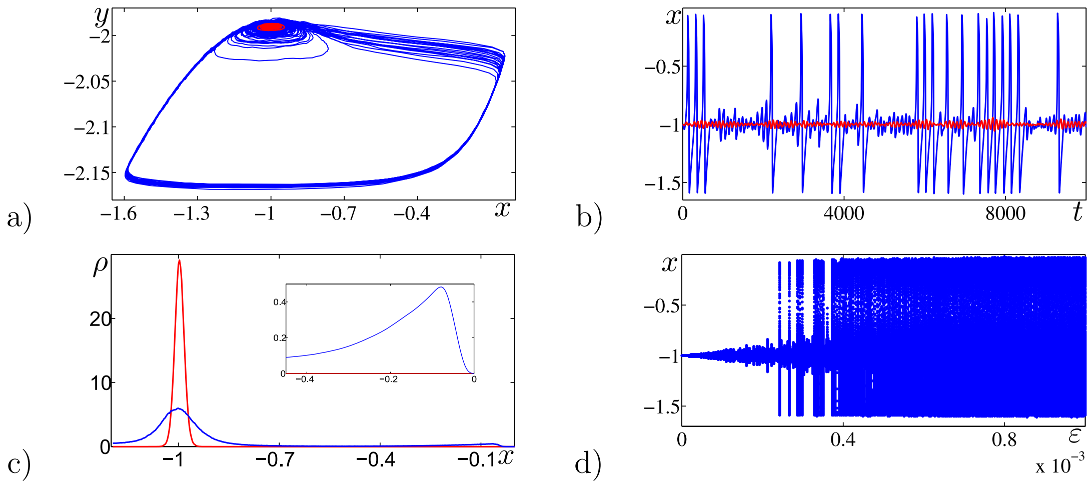

Fig. 5. Stochastic system with $\alpha = 1.98$: (a) random states for $\varepsilon = 0.0001$ (red) and $\varepsilon = 0.0005$ (blue); (b) time series of the variable x; (c) probability density of x; d) x-coordinates of random states versus ε. (For interpretation of the references to colour in this figure legend, the reader is referred to the web version of this article.)

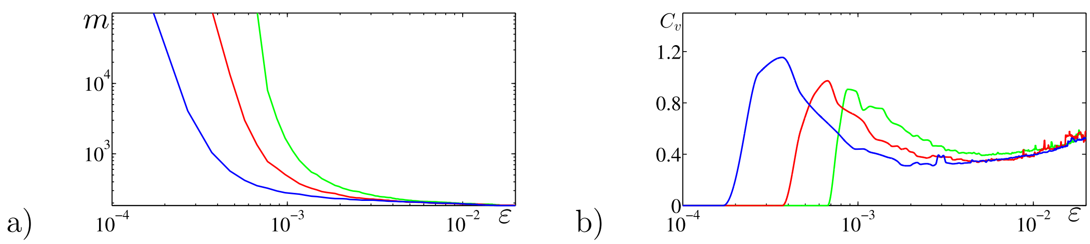

Fig. 6. Statistics of interspike intervals of system (2) with $\alpha = 1.9$ (green), $\alpha = 1.94$ (red), $\alpha = 1.98$ (blue): a) mean values m, b) coefficients of variation C_v. (For interpretation of the references to colour in this figure legend, the reader is referred to the web version of this article.)

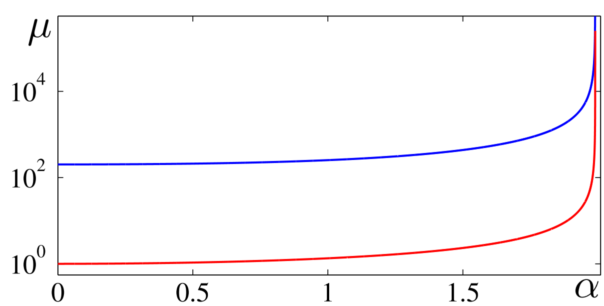

Fig. 7. Eigenvalues $\mu_{1,2}(\alpha)$ of the stochastic sensitivity matrix $W(\alpha)$.

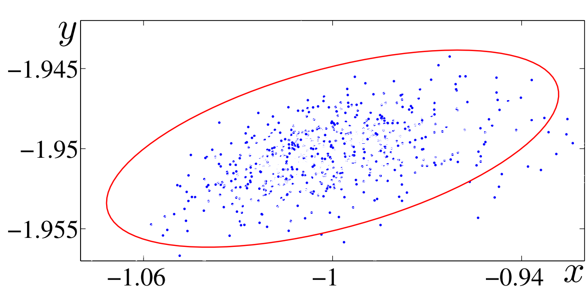

Fig. 8. Confidence ellipse and random states of system (2) with $\alpha = 1.9$, $\varepsilon = 0.0005$ and fiducial probability $P = 0.99$.

Using eigenvalues and eigenvectors of the stochastic sensitivity matrix W, one can easily find a confidence ellipse (see formula (A.3)) for random states distributed near the equilibrium. In Fig. 8, the confidence ellipse and random states of system (2) with $\alpha = 1.9$, $\varepsilon = 0.0005$ are shown. Here, the fiducial probability $P = 0.99$. As can be seen, the ellipse adequately describes the dispersion of random states.

Consider now how confidence ellipses can be used in the parametric analysis of the noise-induced excitement of the stochastic bursting. Results of such analysis are presented in Fig. 9. Here, confidence ellipses are plotted along with deterministic phase trajectories. In Fig. 9(a), for $\alpha = 1.9$, small ellipse corresponds to the noise intensity $\varepsilon = 0.0005$, and large one corresponds to $\varepsilon = 0.0008$. As can be seen from the mutual arrangement of ellipses and deterministic phase trajectories, the small ellipse entirely belongs to the subthreshold zone, and the large ellipse partially occupies the superthreshold zone. This occupation means that random trajectories for $\varepsilon = 0.0008$ can fall into the superthreshold zone and generate large-amplitude spikes.

In Fig. 9(b), for $\alpha = 1.98$, small and large ellipses correspond to the noise intensity $\varepsilon = 0.0002$ and $\varepsilon = 0.0005$, respectively. So, for $\alpha = 1.98$, the generation of the stochastic bursting occurs for smaller noise. These results well agree with the data of direct numerical simulations (see Figs. 4 and 5). Thus, the method of confidence ellipses base on the stochastic sensitivity function technique can be effectively used for the parametric analysis of the transition from the noisy quiescence to the stochastic bursting.

5. Noise-induced transitions to chaos

Along with the study of the changes in amplitude characteristics of stochastic oscillations it is important to consider how noise changes the interior dynamics of stochastic solutions of system (2). The largest Lyapunov exponent Λ is a widely used characteristics of the interior dynamics. In Fig. 10, plots of the function $\Lambda(\varepsilon)$ are shown for different values of the parameter α. As one can see, the common feature of these plots is a presence of the zone of growth with the subsequent slow decrease. This zone of growth

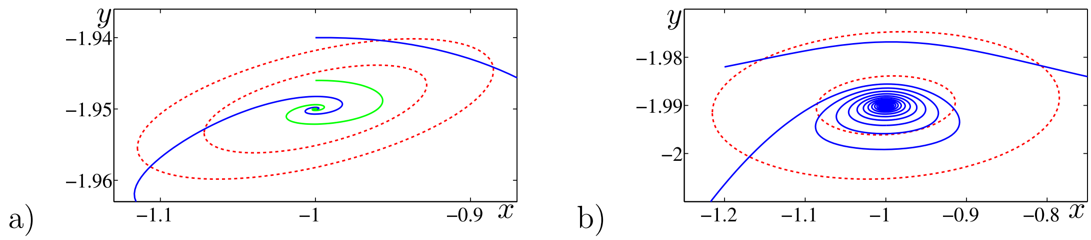

Fig. 9. Confidence ellipses and trajectories of the deterministic system (1) for (a) $\alpha = 1.9$, $\varepsilon = 0.0005$ (small), $\varepsilon = 0.0008$ (large); (b) $\alpha = 1.98$, $\varepsilon = 0.0002$ (small), $\varepsilon = 0.0005$ (large).

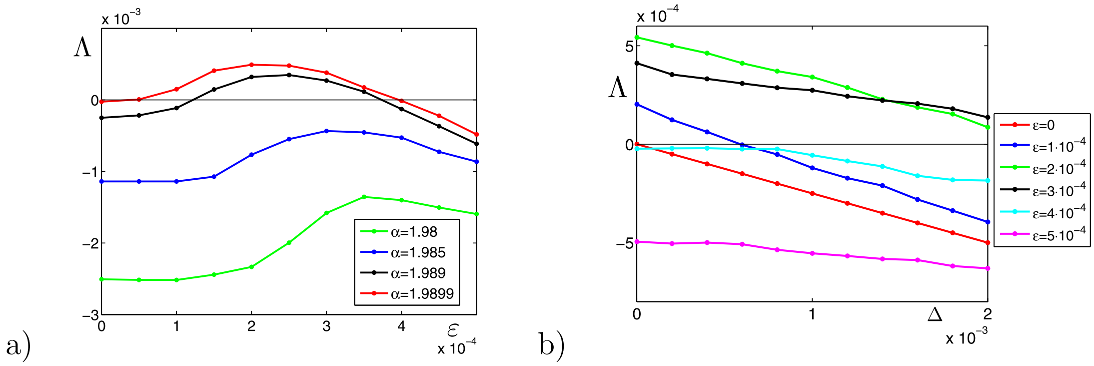

Fig. 10. Largest Lyapunov exponents for system (2): (a) for different α vs noise intensity ε; (b) for different ε vs $\Delta = \alpha^* - \alpha$.

corresponds to the onset of the transitions from small-amplitude stochastic oscillations near the equilibrium to the stochastic bursting with the large-amplitude spiking (compare for $\alpha = 1.98$ green curve in Fig. 10(a) with Figs. 5 and 9). When the parameter α increases and approaches the bifurcation value α^*, the functions $\Lambda(\varepsilon)$ shift up, and partially fall into the zone $\Lambda > 0$. The change of the sign of the largest Lyapunov exponent from minus to plus is commonly interpreted as the stochastic *D*-bifurcation with the transition from order to chaos. As can be seen in Fig. 10, near the Neimark–Sacker bifurcation point, the noise-induced generation of the stochastic bursts is accompanied by the transition of the Rulkov model (2) from order to chaos.

6. Conclusion and discussion

We studied the phenomenon of the noise-induced bursting in the discrete two-dimensional Rulkov neuron model. In the deterministic case, this well-known conceptual model exhibits basic types of the neural activity, such as the quiescence, the tonic spiking and bursting. Mathematically, the diversity of dynamic regimes is connected with different types of attractors. Our interest was focused on the parametric zone near the Neimark–Sacker bifurcation where the equilibrium loses its stability and the closed invariant curves with the Canard-type explosion are born. One of the most remarkable features of the stochastic dynamics of 2D Rulkov model is that even the small noise can generate large-amplitude oscillations in a zone of stable equilibria. In the present paper, this noise-induced excitability was studied by mean values and variations of the interspike intervals. The qualitative change of the form of the probability density (*P*-bifurcation) was revealed. Along with the analysis of direct numerical simulations data, the theoretical approach based on the stochastic sensitivity functions technique and confidence ellipses method was applied. With the help of this technique, the parametric analysis of the transition from the quiescence to the stochastic bursting regime was carried out. It was also shown that such changes in the amplitude of stochastic oscillations are accompanied by the transition from order to chaos (*D*-bifurcation). It is worth noting that our technique is applicable to the analysis of the noise-induced excitability in more complicated multidimensional discrete-time systems.

Acknowledgment

The work was supported by Russian Science Foundation (N 16-11-10098).

Appendix

Consider the following generalized discrete stochastic system

$$x_{t+1} = f(x_t) + \varepsilon\sigma(x_t)\xi_t, \tag{A.1}$$

where x is an n-vector, $f(x)$ is a sufficiently smooth vector-function, $\sigma(x)$ is $n \times m$-matrix, ξ_t is m-dimensional uncorrelated random process with parameters $E\xi_t = 0$, $E\xi_t\xi_t^\top = I$, $E\xi_t\xi_k^\top = 0 (t \neq k)$. Here, I is an identity $m \times m$-matrix. The scalar parameter ε stands for the noise intensity.

Let $\bar{x} = f(\bar{x})$ be an exponentially stable equilibrium of the deterministic system (A.1) with $\varepsilon = 0$ therein. Under the random disturbances, around the equilibrium $\bar{x}$, a probabilistic distribution $p(x, \varepsilon)$ of random states of system (A.2) is formed. For weak noise, this distribution has the Gaussian approximation

$$p(x, \varepsilon) \approx K \exp\left(-\frac{(x - \bar{x}, W^{-1}(x - \bar{x}))}{\varepsilon^2}\right),$$

where the matrix W can be found from the equation [37]

$$W = FWF^\top + Q, \quad F = \frac{\partial f}{\partial x}(\bar{x}), \quad Q = \sigma(\bar{x})\sigma^\top(\bar{x}). \tag{A.2}$$

The stochastic sensitivity matrix W gives a simple description of the response of system (A.1) to random disturbances in the form of confidence ellipses. In two-dimensional case, the confidence ellipse around the equilibrium $\bar{x}$ can be written as

$$(x - \bar{x}, W^{-1}(x - \bar{x})) = 2q^2\varepsilon^2.$$

Here, $q^2 = -\ln(1 - P)$, and P is a fiducial probability. Let the stochastic sensitivity matrix W have eigenvalues μ_1, $\mu_2 > 0$, and corresponding eigenvectors u_1, u_2. For coordinates $z_1 = (x - \bar{x}, u_1), z_2 = (x - \bar{x}, u_2)$, the equation of the confidence ellipse can be written in the canonic form:

$$\frac{z_1^2}{\mu_1} + \frac{z_2^2}{\mu_2} = 2q^2\varepsilon^2. \tag{A.3}$$

References

[1] Rinzel J, Ermentrout GB. Analysis of neural excitability and oscillations. Methods in neuronal modeling. Massachusetts: The MIT Press; 1989.
[2] Izhikevich EM. Dynamical systems in neuroscience: the geometry of excitability and bursting. Massachusetts: The MIT Press; 2007.
[3] Laing C, Lord GJ. Stochastic methods in neuroscience. Oxford: Oxford University Press; 2010.
[4] FitzHugh R. Impulses and physiological states in theoretical models of nerve membrane. Biophys J 1961;1:445–66.
[5] Lindner B, Garcia-Ojalvo J, Neiman A, Schimansky-Geier L. Effects of noise in excitable systems. Phys Rep 2004;392:321–424.
[6] Lindner B, Schimansky-Geier L. Analytical approach to the stochastic Fitzhugh–Nagumo system and coherence resonance. Phys Rev E 1999;60:7270–6.
[7] Pikovsky AS, Kurths J. Coherence resonance in a noise-driven excitable system. Phys Rev Lett 1997;78:775–8.
[8] Bashkirtseva I, Ryashko L. Analysis of excitability for the Fitzhugh—Nagumo model via a stochastic sensitivity function technique. Phys Rev E 2011;83:061109.
[9] Hodgkin AL, Huxley AF. A quantitative description of membrane current and its application to conduction and excitation in nerve. J Physiol 1952;117:500–44.
[10] Guckenheimer J, Oliva RA. Chaos in the Hodgkin–Huxley model. SIAM J Appl Dyn Syst 2002;1:105–14.
[11] Rowat PF, Greenwood PE. The ISI distribution of the stochastic Hodgkin–Huxley neuron. Front Comput Neurosci 2014;8:111.
[12] Che YQ, Wang J, Si WJ. Phase-locking and chaos in a silent Hodgkin–Huxley neuron exposed to sinusoidal electric field. Chaos Solitons Fractals 2009;39:454–62.
[13] Bashkirtseva I, Neiman AB, Ryashko L. Stochastic sensitivity analysis of noise-induced suppression of firing and giant variability of spiking in a Hodgkin–Huxley neuron model. Phys Rev E 2015;91:052920.
[14] Morris C, Lecar H. Voltage oscillations in the barnacle giant muscle fiber. Biophys J 1981;35:193–213.
[15] Liu C, Liu X, Liu S. Bifurcation analysis of a Morris–Lecar neuron model. Biol Cybern 2014;108:75–84.
[16] Ditlevsen S, Samson A. Estimation in the partially observed stochastic Morris–Lecar neuronal model with particle filter and stochastic approximation methods. Ann Appl Stat 2014;8:674–702.
[17] Tateno T, Pakdaman K. Random dynamics of the Morris–Lecar neural model. Chaos 2004;14:511.
[18] Hindmarsh JL, Rose RM. A model of neuronal bursting using three coupled first order differential equations. Proc R Soc B Biol Sci 1984;221:87–102.
[19] Barrio R, Martinez MA, Serrano S, Shilnikov A. Macro- and micro-chaotic structures in the Hindmarsh–Rose model of bursting neurons. Chaos 2014;24:023128.
[20] Barrio R, Lefranc M, Martinez MA, Serrano S. Symbolic dynamical unfolding of spike-adding bifurcations in chaotic neuron models. Europhys Lett 2015;109:20002.
[21] Longtin A. Autonomous stochastic resonance in bursting neurons. Phys Rev E 1997;55:868–76.
[22] Baltanas J, Casado J. Noise-induced resonances in the Hindmarsh–Rose neuronal model. Phys Rev E 2002;65:041915.
[23] Bashkirtseva I, Ryashko L, Slepukhina E. Order and chaos in the stochastic Hindmarsh–Rose model of the neuron bursting. Nonlinear Dyn 2015;82:919–32.
[24] Ibarz B, Casado JM, Sanjuan MAF. Map-based models in neuronal dynamics. Phys Rep 2011;501:1–74.
[25] Rulkov NF. Regularization of synchronized chaotic bursts. Phys Rev Lett 2001;86:183.
[26] Shilnikov AL, Rulkov NF. Origin of chaos in a two-dimensional map modeling spiking-bursting neural activity. Int J Bifurcation Chaos 2003;13:3325–40.
[27] Wang C, Cao H. Parameter space of the Rulkov chaotic neuron model. Commun Nonlinear Sci Numer Simulat 2014;19:2060–70.
[28] Levanova TA, Kazakov AO, Osipov GV, Kurths J. Dynamics of ensemble of inhibitory coupled Rulkov maps. Eur Phys J Special Top 2016;225:147–57.
[29] Boccaletti S, Latora V, Moreno Y, Chavez M, Hwang DU. Complex networks: structure and dynamics. Phys Rep 2006;424:175–308.
[30] Franovic I, Miljkovic V. Functional motifs: a novel perspective on burst synchronization and regularization of neurons coupled via delayed inhibitory synapses. Chaos Solitons Fractals 2011;44:122–30.
[31] Girardi-Schappo M, Tragtenberg MHR, Kinouchi O. A brief history of excitable map-based neurons and neural networks. J Neurosci Methods 2013;220:116–30.
[32] Bashkirtseva I, Ryashko L. Analysis of noise-induced chaos-order transitions in Rulkov model near crisis bifurcations. Int J Bifurcation Chaos 2017;27:1730014.
[33] Mayer-Kress G, Haken H. The influence of noise on the logistic model. J Stat Phys 1981;29:149–71.
[34] Crutchfield JP, Farmer J, Huberman BA. Fluctuations and simple chaotic dynamics. Phys Rep 1982;92:45–82.
[35] Schuster HG. Deterministic chaos. An introduction. Weinheim: Physik-Verlag; 1984.
[36] Lasota A, Mackey MC. Chaos, fractals, and noise: stochastic aspects of dynamics. Berlin: Springer-Verlag; 1994.
[37] Bashkirtseva I, Ryashko L, Tsvetkov I. Sensitivity analysis of stochastic equilibria and cycles for the discrete dynamic systems. DCDIS Seri 2010;17:501–15.
[38] Arnold L. Random dynamical systems. Berlin: Springer; 1998.